

Superconductivity of MgB_2 from Hole-Doped Covalent Bonds

J. M. An and W. E. Pickett

Department of Physics, University of California, Davis CA 95616

(February 8, 2019)

A series of calculations on MgB_2 and related isoelectronic systems indicates that the layer of Mg^{2+} ions lowers the non-bonding B π (p_z) bands relative to the bonding σ ($sp_x p_y$) bands compared to graphite, causing $\sigma \rightarrow \pi$ charge transfer and σ band doping of 0.13 holes/cell. Due to their two dimensionality the σ bands contribute strongly to the Fermi level density of states. Calculated deformation potentials of Γ point phonons identify the B bond stretching modes as dominating the electron-phonon coupling. Superconductivity driven by σ band holes is consistent with the report of destruction of superconductivity by doping with Al.

The dependence of the superconducting critical temperature T_c on structure is unclear after decades of study, and recent discoveries have further confused the issues. In conventional superconductors (the high T_c cuprates comprise a special case) it has been generally thought that high symmetry, preferably cubic, is favorable for higher T_c . This trend has held up in elemental superconductors (Nb, La under pressure, at 9 K and 13 K, respectively), for binaries ($\text{Nb}_3(\text{Al}, \text{Ge})$, 23 K [1]), (pseudo)ternaries such as $(\text{Ba}, \text{K})\text{BiO}_3$, [2] and even fullerene superconductors (T_c to 40 K [3]).

Recently several intriguing counterexamples to this trend have come to light. Semiconducting HfNCl (and ZrNCl) is a van der Waals bonded set of covalent/ionic bonded layers, but superconducts up to 25 K when doped (intercalated) with alkali metals. [4] There is evidence that the surface layer of solid C_{60} becomes superconducting up to 52 K when it is injected to high hole concentrations. [5] And most recently, it is reported that the layered metal/metalloid compound MgB_2 superconducts at ~ 40 K, [6,7] which is by far the highest T_c for a binary system. The B isotope shift of T_c reported by Bud'ko *et al.* [7] and most other early experimental data [8] suggests conventional BCS strong-coupling s-wave phonon pairing. These examples suggest there are important aspects of two dimensionality (2D) for conventional superconductors that are yet to be understood.

A close analogy for MgB_2 , structurally, electronically, and regarding superconductivity, is graphite. Graphite has the same C layer structure as B has in MgB_2 . The layer stacking that occurs in graphite is central to its semimetallic character but is not important in our analogy. Graphite is isoelectronic with MgB_2 – previous studies have established that the Mg atom is effectively ionized. Finally, graphite becomes superconducting up to 5 K, but only when doped (intercalated). [9] Both graphite and MgB_2 have planar sp^2 bonding, and in graphite

it is well established that three of carbon's four valence electrons are tied up in strong σ bonds lying in the graphite plane, and the other electron lies in non-bonding (p_z) π states. Electron doping of graphite, achieved by intercalating alkali atoms between the layers (Na is the most straightforward case) leads to occupation of otherwise unfilled π states and leads to T_c as high as 5 K. MgB_2 , on the other hand, superconducts at ~ 40 K at stoichiometry.

The light masses in MgB_2 enhance the phonon frequency ($\omega_{ph} \propto M^{-1/2}$) that sets the temperature scale of T_c in BCS theory. Even considering this tendency, there must be some *specific feature(s)* that produces such a remarkable T_c , and moreover does so without any d electrons or even the benefit of a density of states (DOS) peak. [10] In this paper we identify this feature: it is the hole doping of the strongly bonding σ bands, resulting in Fermi surface sheets of states that are extremely strongly coupled to the B bond stretching modes. We exploit the similarities between graphite and MgB_2 to build a basic understanding of its electronic structure, and then focus on the differences that are connected to strong electron-phonon (EP) coupling. Although the hole density n_h is small, the strong 2D character of the σ bands leads to a substantial value of the Fermi level density of states $N(\varepsilon_F) \sim m^*/\pi\hbar^2$ that is independent of n_h for strictly 2D bands. This substantial value of $N(\varepsilon_F)$, combined with strong modulation of the σ bands by B displacements and the light mass of B, leads to a strong contribution to EP coupling in spite of small carrier density. This picture further predicts that electron doping by ~ 0.2 carriers per cell will strongly affect T_c adversely, a result that has been reported by Slusky *et al.* [11]

Calculations of the electronic structure have been done using the linearized augmented plane wave (LAPW) method [12] that utilizes a fully general shape of density and potential, as implemented in the WIEN97 code. [13] Experimental lattice constants of $a=3.083$ Å, $c=3.521$ Å were used. LAPW

sphere radii (R) of 2.00 a.u. and 1.65 a.u. were chosen for the Mg and B atoms, respectively, with cut-off $RK_{max}=8.0$, providing basis sets with more than 1350 functions per primitive cell. The generalized gradient approximation exchange-correlation functional of Perdew *et al.* [14] was used in the present work.

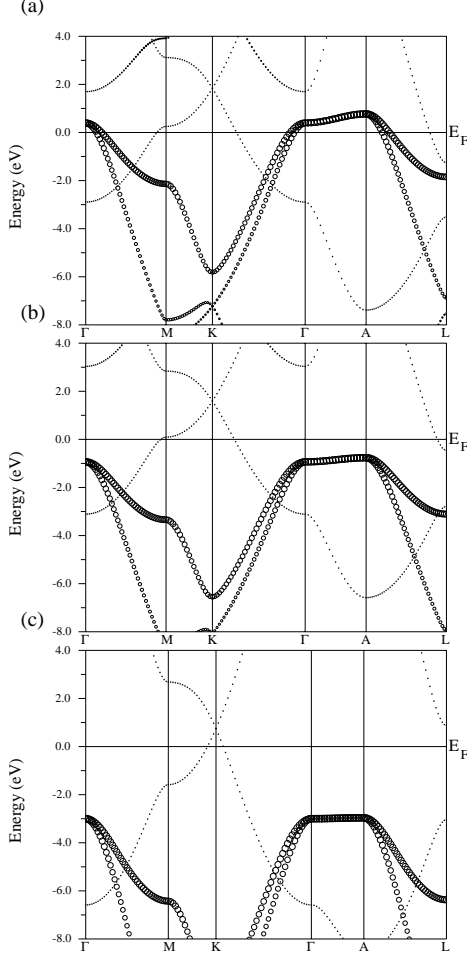


FIG. 1. Band structure along main hexagonal symmetry lines, for (top) MgB_2 , (middle) $\square^{2+}\text{B}_2$, (bottom) primitive graphite C_2 . The planar σ states, highlighted with larger symbols, fall in energy in this progression, and only in MgB_2 are they partially unoccupied.

The band structure of MgB_2 is shown in Fig. 1 (top panel) in comparison with that of graphite (bottom panel) with a single layer per cell (like the B_2 sublattice in MgB_2), and for each two distinct sets of bands are identifiable: the sp^2 (σ) states, and the p_z (π) states. We focus on the σ bands, which are emphasized in Fig. 1. The crucial difference between the band structures is the relative positions of the σ bands. Whereas the σ bonding states are completely filled in graphite, in MgB_2 they are unfilled, with a concentration of 0.067 holes/B atom in cylinders surrounding the Γ -A line of the Brillouin

zone. There are correspondingly more electron carriers in the π bands. This decrease in occupation on the strongly bonding σ bands partially accounts for the greatly increased planar lattice constant of MgB_2 compared to graphite. Our results agree with previous conclusions that MgB_2 can be well characterized by the ionic form $\text{Mg}^{2+}\text{B}_2^{2-}$.

To identify the origin of the relative shift of the σ and π bands by ~ 3.5 eV between graphite and MgB_2 , we have considered a fictitious system $\square^{2+}\text{B}_2$ in which the Mg ion is removed but the two electrons it contributes are left behind (and compensated by a uniform background charge). The band structure, shown in the middle panel of Fig. 1, is very similar, except the energy shift of ~ 1.5 eV downward with respect to MgB_2 completely fills the σ bands. This shift is the result of the attractive Mg^{2+} potential in MgB_2 , which is felt more strongly by the π electrons than by the in-plane σ electrons: the attractive potential of Mg^{2+} between B_2 layers lowers the π bands, resulting in $\sigma \rightarrow \pi$ charge transfer that drives the hole doping of the σ bands. Belashchenko *et al.* [15] have also considered a sequence of materials to come to related conclusions about the band structure, but they did not use isoelectronic systems as has been done here.

While the σ bands are strongly 2D, it is important to establish the magnitude and effects of interplanar coupling. The light hole and heavy hole σ bands in MgB_2 can be modeled realistically in the region of interest (near and above ε_F) with dispersion of the form

$$\varepsilon_k = \varepsilon_0 - \frac{k_x^2 + k_y^2}{2m^*} - 2t_\perp \cos(k_z c), \quad (1)$$

where the planar effective mass m^* is taken to be positive and $t_\perp = 92$ meV is the small dispersion perpendicular to the layers. The light and heavy hole masses are $m_{lh}^*/m=0.20$, $m_{hh}^*/m=0.53$, and the mean band edge is $\varepsilon_0=0.6$ eV. In general the in-plane (v_{xy}) and perpendicular (v_z) Fermi velocities are expected to be strongly anisotropic: $v_{xy} \sim k_F/m^*$, $v_z \sim 2ct_\perp$ where t_\perp is small. The π bands, on the other hand, are essentially isotropic. [10]

Neglecting the k_z dispersion, the 2D hole density of states is constant: $N_h(\varepsilon) = \frac{m_{lh}^* + m_{hh}^*}{\pi \hbar^2} = 0.25$ states/eV-cell. The effect of k_z dispersion is displayed in Fig. 2, where the discontinuity in the quasi-2D DOS is seen to be broadened by $2t_\perp$ and the effect of k_z dispersion extends somewhat further away than $2t_\perp$ from the band edge. The in-plane and perpendicular velocities from the hole bands are also shown in Fig. 2. The in-plane velocity is a distorted version of $v_{xy} \propto \sqrt{\varepsilon_0 - \varepsilon}$ within $4t_\perp$ of the band edge, whereas v_z is comparable very near the band edge but attains the constant value $2c^2 t_\perp^2 =$

3.6×10^7 cm/sec at the Fermi level and below. The anisotropy v_{xy}^2/v_z^2 for the σ bands is about a factor of 4 for MgB₂, but would decrease upon electron doping and increase upon hole doping (Fig. 2).

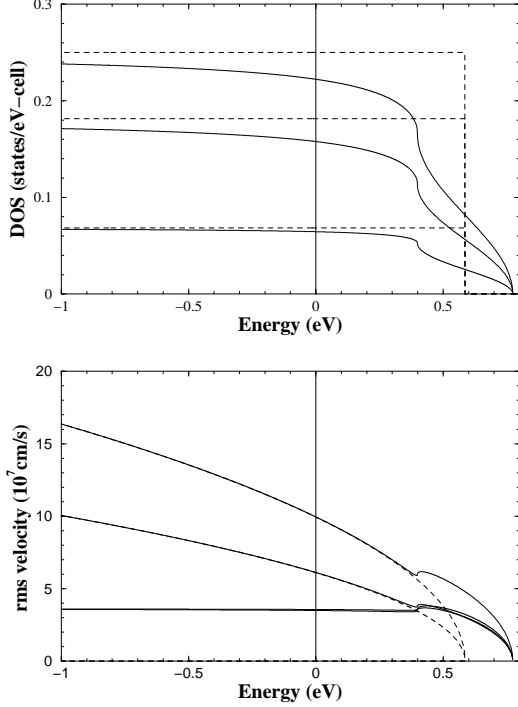


FIG. 2. Top: density of states (solid lines) of the light hole band, the heavy hole band, and the total, for the model of Eq. (1). Note that $N(\epsilon)$ drops very rapidly 0.4 eV above ϵ_F . The dashed lines give the 2D ($t_{\perp}=0$) analogs. Bottom: velocities of the planar σ (hole) bands in MgB₂, compared to their ideal 2D counterparts. The upper two curves are for v_{xy} (light hole, heavy hole). The lower curve is v_z , which happens to track v_{xy} for the heavy hole near the band edge. The zero of energy is at the Fermi level of MgB₂.

If superconductivity is primarily due to the existence of holes in the σ band, and we provide evidence for such a picture below, then the DOS in Fig. 2 suggests that electron doping will decrease T_c . The decrease will be smooth to a doping level corresponding to an increase by 0.4 eV of the Fermi level. Then T_c should drop precipitously with further doping. A rigid band estimate gives a value of $n_{h,cr}=0.08$ electrons necessary to fill the σ bands to the crossover region. Electrons must also be added to the π bands that lie in the same temperature range, making the total doping level $n_{cr} \approx 0.25$ per cell.

Now we address the question of electron-phonon coupling strength. The calculated value of $N(\epsilon_F)=0.71$ states/eV-cell corresponds to a bare specific heat coefficient $\gamma_0 = 1.7$ mJ/mole-K². For context, we note that if the relevant average phonon

frequency is likely to be roughly [10] $\omega \approx 400$ cm⁻¹ ≈ 500 K, and the Coulomb pseudopotential is $\mu^* \approx 0.15$ as typically assumed, application of the Allen-Dynes equation [16] indicates an EP coupling strength $\lambda \sim 1.4$ is required to give $T_c=40$ K. This is a very large value of λ for a metal with only sp electrons; recall that λ is independent of atomic masses. Kortus *et al.* have used the rigid muffin tin approximation [17] to obtain an idea of the coupling strength. However, this approximation is not well justified in sp metals and neglects distinctions between bands of different character that we expect to be crucial for high T_c .

There is fortunately a simple way to identify strong coupling using deformation potentials $\mathcal{D} \equiv \Delta\epsilon_k/\Delta Q$ due to frozen-in phonon modes with mode amplitude Q . [18] The underlying concept is that a phonon that is strongly coupled to Fermi surface states will produce a large shift in ϵ_k for states near the Fermi level. [18] We have studied these deformation potentials for the $k=0$ phonons B_{1g}, E_{2g}, A_{2u}, E_{1u} whose energies, 86, 58, 48, 40 meV respectively, have been calculated by Kortus *et al.* [10]

The resulting band structure for the frozen E_{2g} mode is shown in Fig. 3 along the same symmetry lines as shown in Fig. 1. This mode, and also the B_{1g} mode, involves only out-of-phase motion of the two B atoms in the primitive cell, the first involving vibrations in the plane (bond stretching) and the second perpendicular to the plane. In Fig. 3 the actual rms displacements of $\Delta u_B = 0.057$ Å was used, to provide a clear picture of the effect of EP coupling strength. The E_{2g} phonon strongly splits the σ band nearly uniformly all along the Γ -A line and near ϵ_F , with the “gap” opening $\Delta\epsilon_{gap}/\Delta u_B = 26$ eV/Å; note that it is the square of this quantity that enters λ . In stark contrast, the B_{1g}, A_{2u}, and E_{1u} modes produce no visible effect in the bands; we estimate that their deformation potentials are at least a factor of 25 smaller.

Thus the only significant deformation potential is for the σ bands (π band shifts are always small), and only due to the E_{2g} mode. This one is extremely large, suggesting that non-linear coupling may even be occurring. This strong coupling should be observable as a large E_{2g} linewidth, and the superconducting gap can be expected to be larger on the σ Fermi surface sheets than on the π sheets. It is instructive to estimate the coupling from this mode alone, using the conventional form $\lambda = N_h(\epsilon_F) < I^2 > / M < \omega^2 >$. Applying Eq. (2.34) of Kahn and Allen [18] with $\mathcal{D} = 6.5$ eV/Å (because 2 atoms move to produce the 13 eV/Å shift in eigenvalues), accounting for the two σ bands, and the fact that we are assuming that only $\frac{2}{9}$ of the modes – the E_{2g} ones – couple, the numerator is $0.22 \text{ eV}^{-1} \times ((2/\sqrt{2})\mathcal{D})^2 \times \frac{2}{9} \times 2 \text{ bands} =$

8.2 eV/Å². The denominator is (using the B mass and the E_{2g} frequency) 8.7 eV/Å². This rough estimate gives $\lambda \approx 0.95$. Thus it seems plausible that coupling of the σ band to the bond stretching mode may provide most of the coupling to account for the observed value of T_c. Work is ongoing to quantify the EP coupling strength.

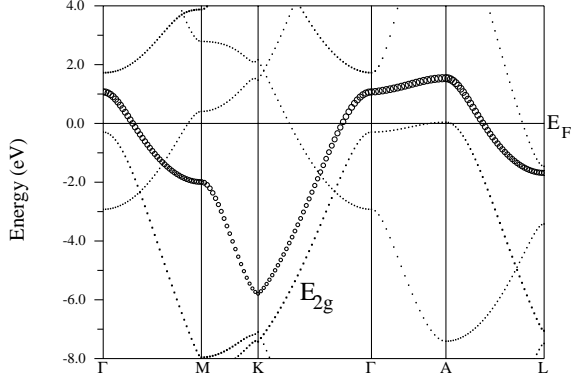


FIG. 3. Band structure with frozen-in E_{2g} mode, only one of the σ bands is highlighted. The E_{2g} phonon breaks the symmetry and splits the σ bands by 1.5 eV along Γ -A.

Now we return briefly to the critical region of electron doping suggested by Fig. 2. Slusky *et al.* have reported [11] a study of the Mg_{1-x}Al_xB₂ system. T_c drops smoothly up to $x=0.1$, beyond which point a two phase mixture of B-rich and Al-rich phases occurs. At $x = 0.25$ and beyond, a single phase, non-superconducting system is restored. This behavior strongly supports our picture of σ bands in MgB₂ that are very strongly coupled to the lattice. Using the rigid band picture, filling them decreases T_c moderately initially, but when the σ bands are filled, the coupling decreases abruptly and T_c vanishes, as observed. Although our results do not bear directly on the two-phase question, we note that this occurs just as the σ bands are filling. At this point $N(\varepsilon_F)$ is dropping, which normally favors stability. The observed instability suggests that a very small density of σ holes that are very strongly coupled to the lattice is what underlies the lattice instability.

To summarize, we identify the “doping” of the planar σ B bands of MgB₂ to be the crucial aspect for the observed high T_c. In spite of the fact that normal state transport may be nearly isotropic, [10,15] two dimensionality is crucial because the contributions of the 2D σ bands to $N(\varepsilon_F)$ is almost independent of the doping level, and the strong covalent nature of the σ bands leads to an extremely large deformation potential. Although Hirsch has also focussed on the hole character of the σ bands, [19] his emphasis is otherwise quite different from that described here.

Positioning of the σ bands at ε_F as in MgB₂ provides extremely strong EP coupling, but only from the bond stretching modes.

W.E.P. is grateful to P. C. Canfield for conversations and for early communication of manuscripts. This work was supported by Office of Naval Research Grant N00017-97-1-0956.

-
- [1] J. R. Gavaler, Appl. Phys. Lett. **23**, 480 (1973).
 - [2] L. F. Mattheiss, E. M. Gyorgy, and D. W. Johnson Jr., Phys. Rev. B **37**, 3745 (1988); R. J. Cava and B. Batlogg, MRS Bulletin **14**, 49 (1989).
 - [3] T. T. M. Palstra *et al.*, Solid State Commun. **93**, 327 (1995).
 - [4] S. Yamanaka *et al.*, Adv. Mater. **9**, 771 (1996); S. Yamanaka, K. Hotehama and H. Kawaji, Nature **392**, 580 (1998); S. Shamoto *et al.*, Physica C **306**, 7 (1998).
 - [5] J. H. Schon, C. Kloc, and B. Batlogg, Nature **408**, 549 (2000).
 - [6] J. Akimitsu, *Symp. on Transition Metal Oxides*, Sendai, January 10, 2001: J. Nagamatsu *et al.* (to be published).
 - [7] S. L. Bud'ko *et al.*, cond-mat/0101463.
 - [8] D. K. Finnemore *et al.*, cond-mat/0102114; G. Rubio-Bollinger *et al.*, cond-mat/0102242; B. Lorenz *et al.*, cond-mat/0102264; P. C. Canfield *et al.*, cond-mat/0102289; A. Sharoni *et al.*, cond-mat/0102325; H. Kotegawa *et al.*, cond-mat/0102334.
 - [9] I. T. Belash *et al.*, Solid State Commun. **64**, 1445 (1987).
 - [10] J. Kortus *et al.*, cond-mat/0101446.
 - [11] J. S. Slusky *et al.*, cond-mat/0102262.
 - [12] D. J. Singh, *Planewaves, Pseudopotentials, and the LAPW Method* (Kluwer Academic, Boston, 1994).
 - [13] P. Blaha, K. Schwarz, and J. Luitz, WIEN97, Vienna University of Technology, 1997. Improved and updated version of the original copyrighted WIEN code, which was published by P. Blaha, K. Schwarz, P. Sorantin, and S. B. Trickey, Comput. Phys. Commun. **59**, 399 (1990).
 - [14] J. P. Perdew *et al.*, Phys. Rev. B **46**, 6671 (1992); J. P. Perdew, K. Burke, and M. Ernzerhof, Phys. Rev. Lett. **77**, 3865 (1996).
 - [15] K. D. Belashchenko, M. van Schilfgaarde, and V. P. Antropov, cond-mat/0102290.
 - [16] P. B. Allen and R. C. Dynes, Phys. Rev. B **12**, 905 (1975).
 - [17] G. D. Gaspari and B. L. Gyorffy, Phys. Rev. Lett. **28**, 801 (1972).
 - [18] F. S. Khan and P. B. Allen, Phys. Rev. B **29**, 3341 (1984).
 - [19] J. E. Hirsch, cond-mat/0102115.